Drugs

Tacrolimus (prograf® injection: Fujisawa Pharmaceutical, Osaka, Japan) was diluted with saline immediately before use. The vehicle solution for the control consisted of polyoxyethylene castor oil (Cremophor EL®, Sigma Chemical CO., St. Louis, MO), ethanol (Wako Pure Chemical Industries Ltd., Osaka, Japan), and saline. This composition was the same as that for the Prograf® injection. Harmine hydrochloride (Sigma Chemical CO., St. Louis, MO) was dissolved in saline. Tacrolimus, vehicle, and harmine were injected intraperitoneally (i.p.) in a volume of 0.5, 0.5, and 0.1 mL/100 g body weight, respectively.

Influence of the Dosing Time of Tacrolimus on Harmine-Induced Tremors and the Concentrations of Serum BUN and Creatinine

Effects of tacrolimus on harmine-induced tremors were evaluated as previously described (Shuto *et al.*, 1998). Tacrolimus (2 mg/kg) or vehicle was injected i.p. once a day for 7 days at 8:00 for the light group or 20:00 for the dark group. Each rat was placed in a screened cage (21.5 × 32× 14 cm) immediately after the 7th injection of tacrolimus to allow adaptation to the new environment and then was introduced to the tremor test. Harmine (10 mg/kg i.p.) was injected 55 min after the final tacrolimus injection. The summed duration of harmine-induced tremors was measured during the 15-min period from 5 to 20 min after harmine administration by the same observer blinded to the pretreatment with tacrolimus or vehicle.

To determine the serum creatinine and BUN concentrations with a Vision analyzer (Abbot Laboratories, Abbot Park, III), blood samples were collected from the rat tail vein 24 h after the final chronic treatment (once a day for 14 days) with tacrolimus (2 mg/kg i.p.) or vehicle at 8:00 or 20:00.

Influence of the Dosing Time of Tacrolimus on Xenograft Survival in Rats Following Xenotransplantation of a Mouse-To-Rat Skin Graft

To make the xenotransplantation model of the mouse-to-rat skin graft, Wistar rats and C57BL/6J mice (15–20 g) were employed as recipients and donors, respectively. The animals were operated on under sodium pentobarbital anesthesia. A square piece (1 cm^2) of skin obtained from the back of the donor mouse was transplanted to where the skin (1 cm^2) was removed from the back of the recipient rat. The skin grafts were protected by gauze with gentacin ointment and bandages for 6 days and rats were housed individually (Shapira *et al.*, 1999).

Xenotransplantation was performed immediately after the first injection of tacrolimus (2 mg/kg i.p.) or vehicle at 8:00 (light group) or 20:00 (dark group). The duration of xenograft survival was determined in each rat with the repeated injection of tacrolimus or vehicle (once a day at 8:00 or 20:00). Rejection was defined as a complete separation of the graft (Shapira *et al.*, 1999).

Pharmacokinetic Influence of the Dosing Time of Tacrolimus

Tacrolimus (2 mg/kg i.p.) was injected once a day at 8:00 (light group) or 20:00 (dark group). Blood samples were obtained from the abdominal aorta at 0.5, 1, 2, 4, 8, 12, and 24 h after a single injection or 24 h after the 7th injection. Tacrolimus concentrations in whole blood were measured with an enzyme immunoassay (IMx; Abbot Laboratories, Abbot Park, III).

Statistical Analysis

Data are expressed as means ± S.E.M. A one-way analysis of variance (ANOVA) followed by the post hoc Sheffe's F-test was used to analyze the concentrations of BUN, creatinine, and tacrolimus. The duration of harmine-induced tremors and that of skin graft survival were evaluated using the Mann–Whitney U-test and log-rank test, respectively. Statistical significance was defined as $P < 0.05$.

RESULTS

Influence of the Dosing Time of Tacrolimus on Harmine-Induced Tremors and the Serum BUN and Creatinine Concentrations

On the basis of the results of preliminary experiments, the dose of harmine was selected to induce a minimal tremor response (the duration of tremors ranged from 0 to 100 s in the light and dark group). Tacrolimus (2 mg/kg i.p., once a day for 7 days) significantly prolonged harmine-induced tremors 2.7-fold compared to the vehicle in the light group ($P < 0.05$), but not in the dark group (Fig. 1). The facilitatory action of tacrolimus on harmine-induced tremors was greater in the light group than dark group (Fig. 1; $P < 0.05$).

In the light group, tacrolimus (2 mg/kg i.p., once a day for 14 days) increased significantly BUN concentrations by 74.7% (Fig. 2(A), $P < 0.01$) and moderately raised creatinine concentrations by 39.5% (Fig. 2(C)). Tacrolimus-affected BUN levels were significantly higher in the light group than dark group ($P < 0.05$). In the dark group, there were only slight differences in the serum BUN and creatinine concentrations between tacrolimus and vehicle treatment (Fig. 2(B) and 2(D)).

Influence of the Dosing Time of Tacrolimus on Xenograft Survival

Figure 3 shows survival curves of the skin xenograft for the light (A) and dark (B) group. The mouse-to-rat skin graft transplanted in the light phase (vehicle; 14.8 ± 0.6 days) survived for a longer period than that transplanted in the dark phase (vehicle; 12.3 ± 0.5 days). In the dark group, tacrolimus (2 mg/kg i.p.) significantly increased the mean survival time by 20% ($P < 0.05$), leading to almost the same levels as those in the light group treated with vehicle or tacrolimus. In the light group, no significant differences were observed between vehicle and tacrolimus treatment.

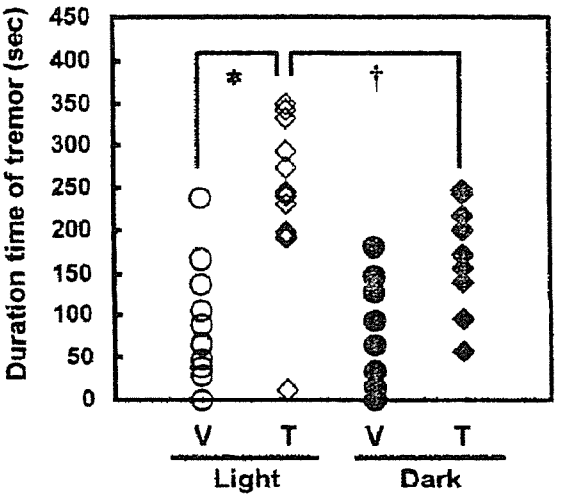

Fig. 1. Influence of the dosing time (8:00 (light) or 20:00 (dark)) of tacrolimus on harmine-induced tremors in rats. The animals were subjected to subchronic treatment with tacrolimus (T) (2 mg/kg i.p.) or vehicle (V) once a day for 7 days. Rats were injected with harmine (10 mg/kg i.p.) 55 min after the final injection of vehicle or tacrolimus. The summed duration of tremors was measured during a 15 min period from 5 to 20 min after harmine injection ($n = 10$–12 per group). $^{*}P < 0.05$; significantly different from the vehicle-treated group. $^{\dagger}P < 0.05$; significantly different from the tacrolimus-treated group in the dark phase.

Pharmacokinetics Influence of the Dosing Time of Tacrolimus After Single or Repeated Injection

The curves for mean tacrolimus concentration versus time after single injections are shown in Fig. 4(A). Tacrolimus levels in whole blood at 1, 4, and 8 h after injection were slightly, although not significantly, higher in the light group than dark group. As shown in Fig. 4(B), the dosing time (light or dark phase) for the repeated injection of tacrolimus had no significant influence on trough levels.

DISCUSSION

The present study demonstrated that the repeated injection of tacrolimus in the light phase (8:00) produced a significantly greater increase than that in the dark phase (20:00) in the duration of harmine-induced tremors and in BUN concentrations in rats. An immunosuppressive effect of tacrolimus on the xenotransplantation of a mouse-to-rat skin graft was apparent in the dark phase but not in the light phase. These findings suggest that treatment in the dark phase (an active phase in the rat diurnal rhythm) ameliorates the neurotoxicity and nephrotoxicity while maintaining the immunosuppressive effect of tacrolimus in rats.

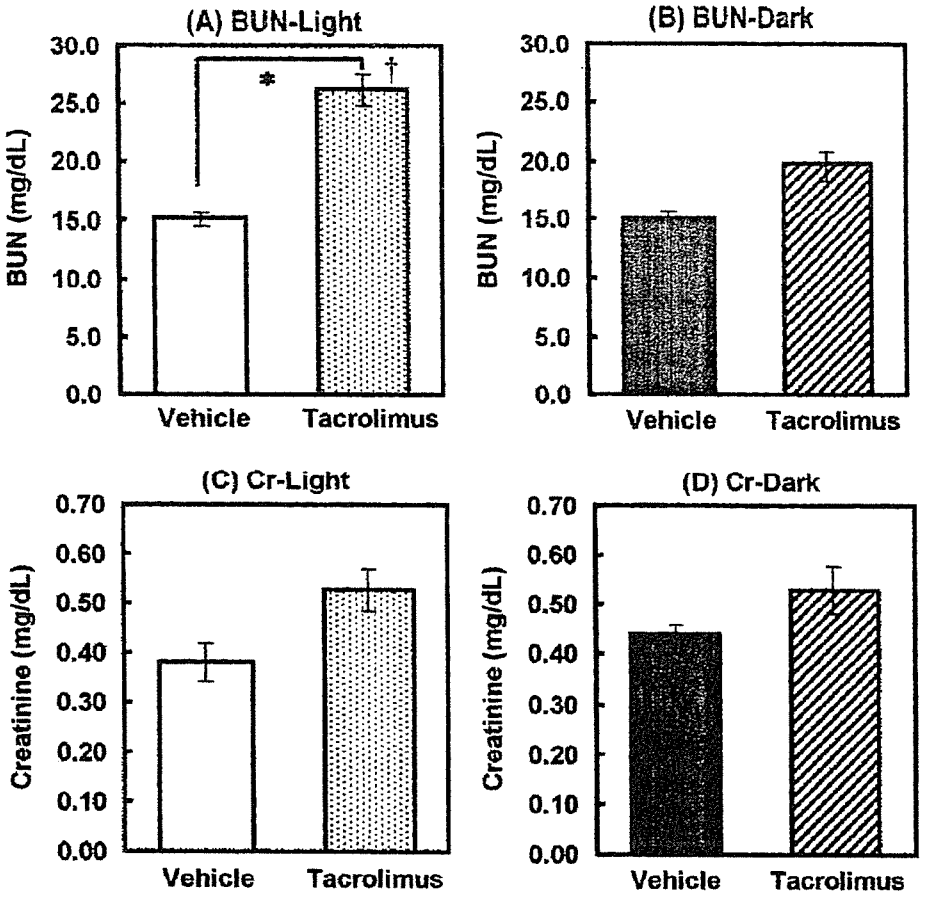

Fig. 2. Influence of the dosing time (8:00 or 20:00) of tacrolimus on the BUN and creatinine concentrations in rats. The animals were subjected to subchronic treatment with tacrolimus (2 mg/kg i.p.) or vehicle once a day for 14 days. Blood samples were collected from the tail vein 24 h after the final tacrolimus injection. Values represent the means ± S.E.M. for 5–7 rats. (A) The BUN concentrations in the light group (BUN-light); (B) The BUN concentrations in the dark group (BUN-dark); (C) The creatinine concentrations in the light group (Cr-light); (D) The creatinine concentrations in the dark group (Cr-dark). $^{**}P < 0.01$; significantly different from the vehicle-treated group. $^{\dagger}P < 0.05$; significantly different from the tacrolimus-treated group in the dark phase.

No chronopharmacological research has been published concerning immunosuppressant-induced neurotoxicity. The present study is the first to provide evidence that a facilitatory action of tacrolimus on harmine-induced tremors shows a diurnal rhythm with a potent effect in the light phase in rats. Harmine is reported to induce tremors by activating serotonergic neurons and inhibiting dopaminergic neurons (Kawanishi *et al.*, 1981). Shuto *et al.* (1998) demonstrated that cyclosporine facilitates serotonergic neural activity to accelerate harmine-induced tremors. This acceleration appeared to be involved in an inhibition of γ-aminobutyric acid neural activity and receptors (Shuto *et al.*, 1999; Tominaga *et al.*, 2001). The precise mechanisms by which tacrolimus neurotoxicity exhibits a diurnal rhythm remains to be determined.

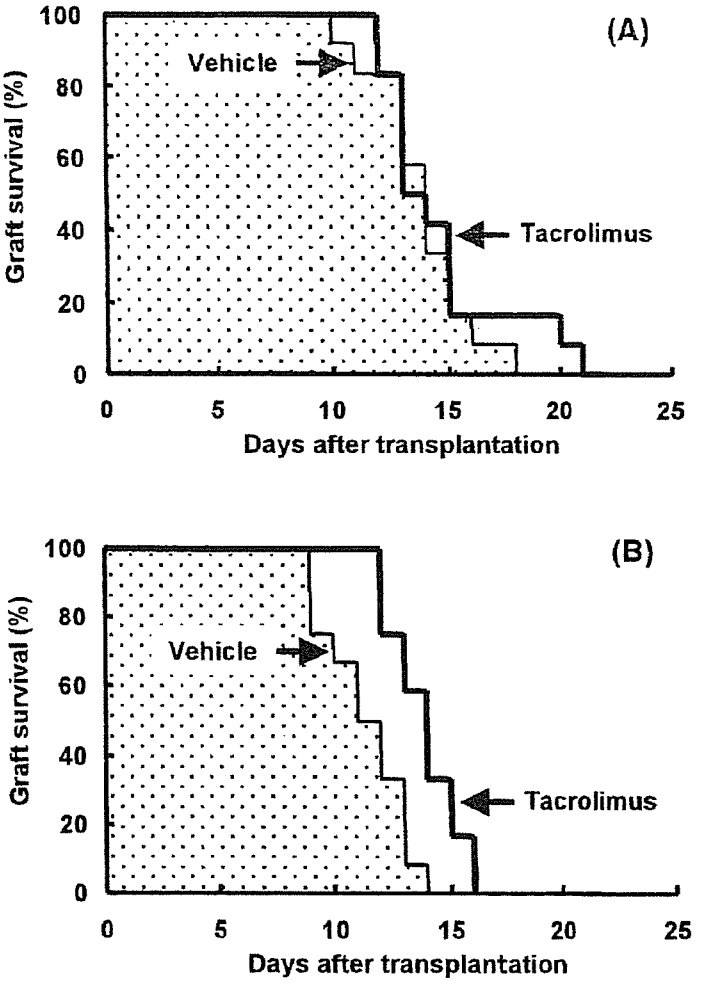

Fig. 3. Influence of the dosing time (8:00 (A) and 20:00 (B)) of tacrolimus on the survival of skin xenografts in a mouse-to-rat skin xenotransplantation model. The animals were subjected to chronic treatment with tacrolimus (2 mg/kg i.p., thick line) or vehicle (thin line and dotted area) once a day until rejection of the graft occurred. Rejection was defined as a complete separation of the graft in each rat. Data are expressed as the percentage of rats in which the graft survived in each group (12 rats each). $^{*}P < 0.05$; significantly different from the vehicle-treated group.

The dosing time-dependent nephrotoxicity of tacrolimus in rats was previously reported by Fujimura and Ebihara (1994). Contrary to our findings, they showed that the tacrolimus-induced elevation in the BUN and creatinine levels was more prominent in the dark phase than in the light phase in rats. Their pharmacokinetic results suggested that an aggravation of renal function induced by tacrolimus in the dark phase is closely associated with the high concentrations of tacrolimus in whole blood in the dark phase. This diurnal rhythm was not observed in the present pharmacokinetic study. The discrepancy in these findings may be due to the different route of administration (an intraperitoneal route in our study versus an oral route

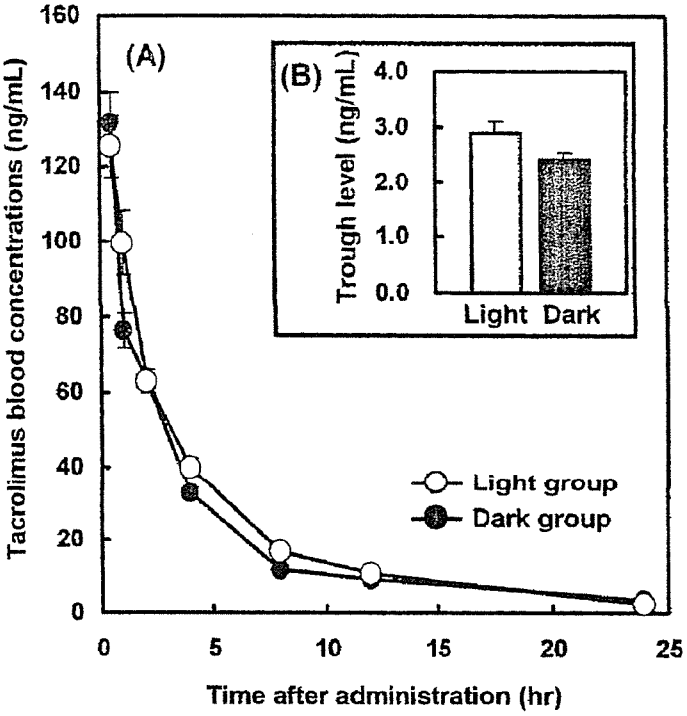

Fig. 4. The pharmacokinetic influence of the dosing time (8:00 (light) or 20:00 (dark)) of tacrolimus (2 mg/kg i.p.) after a single (A) or repeated (B) injection. Blood samples were obtained from the abdominal aorta at 0.5, 1, 2, 4, 8, 12, and 24 h after a single injection or 24 h after repeated injection (once a day for 7 days). Values represent means ± S.E.M. for 5–6 rats.

in Fujimura's study). In the oral administration of tacrolimus, the maximum concentration or area under the concentration–time curve (AUC) of tacrolimus was significantly increased when tacrolimus was given in the morning in humans or in the dark phase in nocturnal rodents (Fujimura *et al.*, 1993, Min *et al.*, 1996, Uchida *et al.*, 1999). These phenomena seem to be caused by several diurnal rhythm-related variables including food ingestion, gastric emptying time, gastric motility, secretion of bile acid, blood flow to the gastrointestinal tract, and gastrointestinal perfusion. In the present study, the dosing time-dependent influences are not involved in tacrolimus absorption, since tacrolimus was intraperitoneally administered. Interestingly, the AUC of tacrolimus on continuous intravenous administration in humans showed no differences between daytime and nighttime (Satoh *et al.*, 2001). This is consistent with our results suggesting that the pharmacokinetic features of tacrolimus following parenteral administration probably indicate no circadian variation. Therefore, the pharmacokinetic factors may be excluded from the mechanisms of diurnal changes in tacrolimus-induced toxicity and efficacy in the present study. The possibility that the distribution of tacrolimus in the kidney and brain has diurnal variations remains to be examined.

Calcineurin inhibitors including tacrolimus and cyclosporine exert an immunosuppressive action due to the inhibition of interleukin (IL)-2 transcription, leading

to T cell inactivation (Liu, 1993; Wiederrecht *et al.*, 2000). Since a diurnal rhythm exists in the secretion of IL-2 or the number of T cells (Born *et al.*, 1997; Palm *et al.*, 1996), the immunosuppressive effects of calcineurin inhibitors are speculated to depend on the dosing time during the day. In the present study, the administration of tacrolimus in the dark phase significantly prolonged the survival time of skin grafts in the xenograft transplantation model. These findings were supported by a report concerning the effect of cyclosporine on a murine heart allograft model (Cavallini *et al.*, 1983). The efficacy of tacrolimus or cyclosporine is likely to increase when the agent is administered in the dark phase in the rodents.

In conclusion, we provided evidence that treatment in the active phase ameliorates the neurotoxicity and nephrotoxicity while maintaining the immunosuppressive effect of tacrolimus in rats. The present findings have important implications for therapeutic approaches to avoid tacrolimus-induced neurotoxicity and nephrotoxicity.

ACKNOWLEDGMENTS

We thank Y. Isotani and K. Toda for assistance. This work was supported in part by a Grant-in-aid for Scientific Research ((B)(2) 14370789) from the Ministry of Education, Culture, Sports, Science, and Technology (MEXT), Japan and by funds (No.: 031001) from the Central Research Institute of Fukuoka University.

REFERENCES

Bobadilla, N. A., Gamba, G., Tapia, E., Garcia-Torres, R., Bolio, A., López-Zetina, P., and Herrera-Acosta, J. (1998). Role of NO in cyclosporin nephrotoxicity: Effects of chronic NO inhibition and NO synthases gene expression. *Am. J. Physiol.* **274:**F791–F798.

Born, J., Lange, T., Hansen, K., Mölle, M., and Fehm, H. L. (1997). Effects of sleep and circadian rhythm on human circulating immune cells. *J. Immunol.* **158:**4454–4464.

Brandenberger, G., Follenius, M., Goichot, B., Saini, J., Spiegel, K., Ehrhart, J., and Simon, C. (1994). Twenty-four-hour profiles of plasma renin activity in relation to the sleep-wake cycle. *J. Hypartens.* **12:**277–283.

Cardinali, D. P., and Golombek, D. A. (1998). The rhythmic GABAergic system. *Neurochem. Res.* **23:**607–614.

Cavallini, M., Magnus, G., Halberg, F., Tao, L., Field, M. Y., Sibley, R., Najarian, J. S., and Sutherland, D. E. R. (1983). Benefit from circadian timing of cyclosporine revealed by delay of rejection of murine heart allograft. *Transplant. Proc.* **15**(Suppl. 1):2960–2966.

European FK506 Multicentre Liver Study Group. (1994). Randomised trial comparing tacrolimus (FK506) and cyclosporin in prevention of liver allograft rejection. *Lancet.* **344:**423–428.

Fujimura, A., and Ebihara, A. (1994). Administration time-dependent toxicity of a new immunosuppressive agent, tacrolimus (FK506). *Life Sci.* **55:**485–490.

Fujimura, A., Shiga, T., Ohashi, K., and Ebihara, A. (1993). Chronopharmacokinetic study of a new immunosuppressive agent, FK506, in mice. *Jpn. J. Pharmacol.* **61:**137–139.

Fujisaki, Y., Yamauchi, A., Dohgu, S., Sunada, K., Yamaguchi, C., Oishi, R., and Kataoka, Y. (2002). Cyclosporine A-increased nitric oxide production in the rat dorsal hippocampus mediates convulsions. *Life Sci.* **72:**549–556.

Hutson, P. H., Sarna, G. S., and Curzon, G. (1984). Determination of daily variations of brain 5-hydroxytryptamine and dopamine turnovers and of the clearance of their acidic metabolites in conscious rats by repeated sampling of cerebrospinal fluid. *J. Neurochem.* **43:**291–293.

Hwang, Y. S., Hsieh, T. J., Lee, Y. J., and Tsai, J. H. (1998). Circadian rhythm of urinary endothelin-1 excretion in mild hypertensive patients. *Am. J. Hypertens.* **11:**1344–1351.

Ikesue, H., Kataoka, Y., Kawachi, R., Dohgu, S., Shuto, H., and Oishi, R. (2000). Cyclosporine enhances α1-adrenoceptor-mediated nitric oxide production in C6 glioma cells. *Eur. J. Pharmacol.* **407:**221–226.

Isram, M., Burke, J. F., Jr., McGowan, T. A., Zhu, Y., Dunn, S. R., McCue, P., Kanalas, J., and Sharma, K. (2001). Effect of anti-transforming growth factor-beta antibodies in cyclosporine-induced renal dysfunction. *Kidney Int.* **59:**498–506.

Kawanishi, K., Hashimoto, Y., Fujiwara, M., Kataoka, Y., and Ueki, S. (1981). Pharmacological characteristics of abnormal behavior induced by harmine with special reference to tremor in mice. *J. Pharm. Dyn.* **4:**520–527.

Kupferman, J. C., Beaudoin, R., Carr, R., Hay, D., Casellas, D., Kaskel, F. J., and Moore, L. C. (1994). Activation of the renal renin-angiotensin system by cyclosporine A and FK 506 in the rat. *Transplant. Proc.* **26:**2891–2893.

Lanese, D. M., and Conger J. D. (1993). Effects of endothelin receptor antagonist on cyclosporine-induced vasoconstriction in isolated rat renal arterioles. *J. Clin. Invest.* **91:**2144–2149.

Lanese, D. M., Falk, S. A., and Conger J. D. (1994). Sequential agonist activation and site-specific mediation of acute cyclosporine constriction in rat renal arterioles. *Transplantation* **58:**1371–1378.

Levi, F., Zidani, R., and Misset, J. L. (1997). Randomised multicentre trial of chronotherapy with oxaliplatin, fluorouracil, and folinic acid in metastatic colorectal cancer. *Lancet* **350:**681–686.

Liu, J. (1993). FK506 and cyclosporin, molecular probes for studying intracellular signal transduction. *Immunol. Today* **14:**290–295.

Min, D. I., Chen, H. Y., Fabrega, A., Ukah, F. O., Wu, Y. M., Corwin, C., Ashton, M. K., and Martin, M. (1996). Circadian variation of tacrolimus disposition in liver allograft recipients. *Transplantation* **62:**1190–1192.

Ohdo, S., Koyanagi, S., Suyama, H., Higuchi, S., and Aramaki, H. (2001). Changing the dosing schedule minimizes the disruptive effects of interferon on clock function. *Nat. Med.* **7:**356–360.

Palm, S., Postler, E., Hinrichsen, H., Maier, H., Zabel, P., and Kirch, W. (1996). Twenty-four-hour analysis of lymphocyte subpopulations and cytokines in healthy subjects. *Chronobiol. Int.* **13:**423–434.

Satoh, S., Tada, H., Tachiki, Y., Tsuchiya, N., Shimoda, N., Akao, T., Sato, K., Habuchi, T., Suzuki, T., and Kato, T. (2001). Chrono and clinical pharmacokietic study of tacrolimus in continuous intravenous administration. *Int. J. Urol.* **8:**353–358

Shapira, O. M., Rene, H., Lider, O., Pfeffermann, R. A., Shemin, R. J., and Cohen, I. R. (1999). Prolongation of rat skin and cardiac allograft survival by low molecular weight heparin. *J. Surg. Res.* **85:**83–87.

Shuto, H., Kataoka, Y., Fujisaki, K., Nakao, T., Sueyasu, M., Miura, I., Watanabe, Y., Fujiwara, M., and Oishi, R. (1999). Inhibition of GABA system involved in cyclosporine-induced convulsions. *Life Sci.* **65:**879–887.

Shuto, H., Kataoka, Y., Kanaya, A., Matsunaga, K., Sueyasu, M., and Oishi, R. (1998). Enhancement of serotonergic neural activity contributes to cyclosporine-induced tremors in mice. *Eur. J. Pharmacol.* **341:**33–37.

Snyder, S. H., Sabatini, D. M., Lai, M. M., Steinet, J. P., Hamilton, G. S., and Suzdak, P. D. (1998). Neuronal actions of immunophilin ligands. *Trends Pharmacol. Sci.* **19:**21–26.

Steiner, J. P., Dawson, T. M., Fotuhi, M., and Snyder, S. H. (1996). Immunophilin regulation of neurotransmitter release. *Mol. Med.* **2:**325–333.

The U.S. Multicenter FK506 Liver Study Group. (1994). A comparison of tacrolimus (FK 506) and cyclosporine for immunosuppression in liver transplantation. *N. Engl. J. Med.* **331:**1110–1115.

Tominaga, K., Yamauchi, A., Shuto, H., Niizeki, M., Makino, K., Oishi, R., and Kataoka, Y. (2001). Ovariectomy aggravates convulsions and hippocampal γ-aminobutyric acid inhibition induced by cyclosporin A in rats. *Eur. J. Pharmacol.* **430:**243–249.

Uchida, H., Kobayashi, E., Ogino, Y., Mizuta, K., To, H., Okabe, R., Hashizume, K., and Fujimura, A. (1999). Chronopharmacology of tacrolimus in rats: Toxicity and efficacy in a mouse-to-rat intestinal transplant model and its pharmacokinetic profile. *Transplant. Proc.* **31:**2751–2753.

Wiederrecht, G., Lam, E., Hung, S., Martin, M., and Sigal, N. (2000). The mechanism of action of FK-506 and cyclosporin A. *Ann. N. Y. Acad. Sci.* **696:**9–19.

Available online at www.sciencedirect.com

SCIENCE DIRECT®

European Journal of Pharmacology 505 (2004) 51–59

ELSEVIER

ejp

www.elsevier.com/locate/ejphar

Nitric oxide mediates cyclosporine-induced impairment of the blood–brain barrier in cocultures of mouse brain endothelial cells and rat astrocytes

Shinya Dohgu[a], Atsushi Yamauchi[a], Shinsuke Nakagawa[b], Fuyuko Takata[a], Mamiko Kai[a], Takashi Egawa[a], Mikihiko Naito[c], Takashi Tsuruo[c], Yasufumi Sawada[d], Masami Niwa[b], Yasufumi Kataoka[a,*]

[a]*Department of Pharmaceutical Care and Health Sciences, Faculty of Pharmaceutical Sciences, Fukuoka University, 8-19-1 Nanakuma, Jonan-ku, Fukuoka 814-0180, Japan*

[b]*Department of Pharmacology 1, Nagasaki University Graduate School of Biomedical Sciences, 1-12-4 Sakamoto, Nagasaki 852-8523, Japan*

[c]*Institute of Molecular and Cellular Biosciences, University of Tokyo, Bunkyo-ku, Tokyo, 113-0032, Japan*

[d]*Department of Medico-Pharmaceutical Sciences, Graduate School of Pharmaceutical Sciences, Kyushu University, 3-1-1 Maidashi, Higashi-ku, Fukuoka 812-8582, Japan*

Received 8 October 2004
Available online 30 October 2004

Abstract

The present study was designed to clarify the involvement of nitric oxide (NO) signaling in the adverse effect of cyclosporine on the blood–brain barrier. Cyclosporine increased the permeability of sodium-fluorescein and the cellular accumulation of rhodamine 123, a substrate of P-glycoprotein, in mouse brain endothelial (MBEC4) cells. This effect was markedly enhanced two- to threefold when MBEC4 cells were cocultured with rat astrocytes or C6 glioma cells. Direct and continuous electrochemical measurement of NO demonstrated that cyclosporine dose-dependently increased histamine- and phenylephrine-evoked NO production in MBEC4 cells and astrocytes, respectively. A NO synthase inhibitor (N^G-monomethyl-L-arginine) blocked slightly and markedly cyclosporine-induced impairment of the endothelial barrier in the monolayer and coculture system, respectively. These findings suggest that cyclosporine impairs the brain endothelial barrier function by accelerating NO production in the brain endothelial and astroglial cells. This event may be interpreted as triggering the occurrence of cyclosporine neurotoxicity.

Keywords: Cyclosporine; Neurotoxicity; NO (nitric oxide); Blood–brain barrier; Permeability; P-glycoprotein

1. Introduction

Cyclosporine, a cyclic 11-amino acid peptide, is widely used as a potent immunosuppressant to prevent allograft rejection in solid organ transplantation and in fatal graft-vs.-host disease after bone marrow transplantation, and to treat various autoimmune diseases including rheumatoid arthritis (Kahan, 1989). Despite its high efficacy, cyclosporine has adverse effects including renal dysfunction, cardiovascular disorders, gastrointestinal disorders and neurological complications. These events occur with a relatively high frequency (20–40%) in organ-transplanted patients (Gijtenbeek et al., 1999; Pirsch et al., 1997; U.S. Group, 1994).

The entry of cyclosporine into the brain is prevented by the tight junctions and P-glycoprotein, a multi-drug efflux pump, of the brain microvascular endothelial cells. But the adverse neurological effects of cyclosporine, including tremors, seizures and encephalopathy, strongly suggest the possibility of cyclosporine transport across the blood–brain

* Corresponding author. Tel./fax: +81 92 862 2696.
E-mail address: ykataoka@cis.fukuoka-u.ac.jp (Y. Kataoka).

0014-2999/$ - see front matter © 2004 Elsevier B.V. All rights reserved.
doi:10.1016/j.ejphar.2004.10.027

barrier. We previously reported that cyclosporine produced convulsions by inhibiting γ-aminobutyric acid (GABA)-ergic neural activity and binding properties of the $GABA_A$ receptor (Shuto et al., 1999). The inhibition of GABAergic neurotransmission by cyclosporine may lead to an activation of serotonergic neural activity and consequently produce tremors (Shuto et al., 1998). These findings in vivo are considered to be due to a direct action of cyclosporine transported across the blood–brain barrier rather than an indirect effect through the periphery. In fact, we demonstrated that cyclosporine at a high concentration decreased the function and expression of P-glycoprotein in brain capillary endothelial cells (Kochi et al., 1999; 2000). The blood–brain barrier is primarily formed by brain capillary endothelial cells, which are closely sealed by tight junctions (Partridge, 1999). P-glycoprotein is abundantly expressed in the brain endothelial cells and limits the accumulation of many hydrophobic molecules and toxic substances in the brain (Schinkel, 1999). Recently, we demonstrated that nitric oxide (NO) increased the permeability and inhibited the P-glycoprotein efflux pump of brain capillary endothelial cells, suggesting that NO impairs the dynamic regulation of the blood–brain barrier function (Yamauchi et al., in press). Astrocytes and pericytes are cellular components of the blood–brain barrier. Astrocytes surround the cerebral capillaries and regulate blood–brain barrier function through cell-to-cell contact and secretion of soluble factors (Terasaki et al., 2003).

The present study was designed to clarify the involvement of NO signaling in the adverse effect of cyclosporine on the blood–brain barrier. We first evaluated the effect of cyclosporine on the permeability and the P-glycoprotein function of mouse brain endothelial (MBEC4) cells alone and cocultured with rat astrocytes or C6 glioma cells. Second, the effect of cyclosporine on the stimulation-evoked NO production was examined in MBEC4 cells and rat astrocytes using direct electrochemical NO monitoring.

2. Materials and methods

2.1. Materials

Cyclosporine was kindly supplied by Novartis Pharma (Bazel, Switzerland). Sodium fluorescein (Na-F, MW 376), rhodamine 123, phenylephrine hydrochloride, histamine, L-arginine and N^G-monomethyl-L-arginine (L-NMMA) were purchased from Sigma (St. Louis, MO, USA). Culture medium and subculture reagents were obtained from Invitrogen (Carlsbad, CA, USA). All remaining reagents of analytical grade were purchased from Wako (Osaka, Japan).

2.2. Animals

Wistar rats aged 3 days old were used in this study. All the procedures involving experimental animals adhered to the law (No. 105) and notification (No. 6) of the Japanese Government, and were approved by the Laboratory Animal Care and Use Committee of Fukuoka University.

2.3. Cell culture

MBEC4 cells, which were isolated from BALB/c mouse brain cortices and immortalized by SV40-transformation (Tatsuta et al., 1992), were cultured in Dulbecco's modified Eagle's medium (DMEM) supplemented with 10% fetal bovine serum, 100 units/ml penicillin and 100 μg/ml streptomycin. C6 glioma cells (JCRB9096, Health Science Research Resources Bank, Osaka, Japan) were cultured in DMEM supplemented with 10% fetal calf serum, and 50 μg/ml gentamicin. Newborn rat astrocytes were isolated according to the method of McCarthy and de Vellis (1980) and Sastradipura et al. (1998) with a slight modification. Briefly, the cerebral cortex from 3-day-old rats was minced and treated with papain (90 units/ml; Worthington, Lakewood, NJ) and DNase I (2000 units/ml; Sigma) at 37 °C for 15 min. The mechanically dissociated cells were seeded into plastic flasks in DMEM supplemented with 10% fetal bovine serum, 100 units/ml penicillin and 100 μg/ml streptomycin. After 10–14 days in culture, floating cells and weakly attached cells on the mixed primary cultured cell layer were removed by vigorous shaking of the flask. Then, astrocytes on the bottom of the culture flask were trypsinized and seeded into new culture flasks. The primary cultured astrocytes were maintained in DMEM. They were grown in a humidified atmosphere of 5% CO_2/95% air at 37 °C.

The preparation of the in vitro blood–brain barrier models has been described previously (Dohgu et al., 2000). In brief, C6 cells or rat astrocytes (40,000 cells/cm^2) were first cultured on the outside of the collagen-coated polycarbonate membrane (3.0 μm pore size) of the Transwell™ insert (12-well type, Costar, MA, USA) directed upside down in the well. Two days later, MBEC4 cells (42,000 cells/cm^2) were seeded on the inside of the insert placed in the well of the 12-well culture plate (Costar) (C6 coculture and rat astrocyte coculture). The monolayer system was also made with MBEC4 cells alone (MBEC4 monolayer).

2.4. Treatment with cyclosporine and nitric oxide (NO) synthase inhibitor

Cyclosporine was first dissolved in ethanol and diluted with serum-free culture medium (0.1% as the final ethanol concentration). MBEC4 cells were cultured for 3 days, and these inserts were washed three times with serum-free medium. Then cells were exposed to 1–5 μM cyclosporine injected into the inside of the insert (luminal side) for 12 h. When the effect of NO synthase (NOS) inhibitor was examined, L-NMMA (1 mM) was loaded both inside and outside of the insert (luminal and abluminal side). In

parallel, cells were treated with serum-free medium containing the corresponding amount of ethanol as the vehicle.

2.5. Paracellular transport of Na-F

To initiate the transport experiments, the medium was removed and MBEC4 cells were washed three times with Krebs–Ringer buffer (118 mM NaCl, 4.7 mM KCl, 1.3 mM $CaCl_2$, 1.2 mM $MgCl_2$, 1.0 mM NaH_2PO_4, 25 mM $NaHCO_3$, and 11 mM D-glucose, pH 7.4). Krebs–Ringer buffer (1.5 ml) was added to the outside of the insert (abluminal side). Krebs–Ringer buffer (0.5 ml) containing 100 μg/ml of Na-F was loaded on the luminal side of the insert. Samples (0.5 ml) were removed from the abluminal chamber at 10, 20, 30 and 60 min and immediately replaced with fresh Krebs–Ringer buffer. Aliquots (5 μl) of the abluminal medium were mixed with 200 μl of Krebs–Ringer buffer and then the concentration of Na-F was determined using a fluorescence multiwell plate reader (Ex(λ) 485 nm; Em(λ) 530 nm) (CytoFluor Series 4000, PerSeptive Biosystems, Framingham, MA, USA). The permeability coefficient and clearance were calculated according to the method described by Dehouck et al. (1992). Clearance was expressed as microliters (μl) of tracer diffusing from the luminal to abluminal chamber and was calculated from the initial concentration of tracer in the luminal chamber and final concentration in the abluminal chamber: Clearance (μl)=$[C]_A \times V_A/[C]_L$ where $[C]_L$ is the initial luminal tracer concentration, $[C]_A$ is the abluminal tracer concentration and V_A is the volume of the abluminal chamber. During a 60-min period of the experiment, the clearance volume increased linearly with time. The average volume cleared was plotted vs. time, and the slope was estimated by linear regression analysis. The slope of clearance curves for the MBEC4 monolayer or coculture systems was denoted by PS_{app}, where PS is the permeability-surface area product (in μl/min). The slope of the clearance curve with a control membrane was denoted by $PS_{membrane}$. In the coculture system, the control membrane is the C6 cell- or rat astrocyte-layered membrane. The real PS value for the MBEC4 monolayer and the coculture system (PS_{trans}) was calculated from $1/PS_{app}=1/PS_{membrane}+1/PS_{trans}$. The PS_{trans} values were divided by the surface area of the Transwell inserts to generate the permeability coefficient (P_{trans}, in cm/min).

2.6. Functional activity of P-glycoprotein

The functional activity of P-glycoprotein was determined by measuring the cellular accumulation of rhodamine 123 (Sigma) according to the method of Fontaine et al. (1996). MBEC4 cells were washed three times with assay buffer (143 mM NaCl, 4.7 mM KCl, 1.3 mM $CaCl_2$, 1.2 mM $MgCl_2$, 1.0 mM NaH_2PO_4, 10 mM HEPES, and 11 mM D-glucose, pH 7.4). In both coculture systems, C6 cells and rat astrocytes on the outside of the membrane were removed with a cell scraper. MBEC4 cells were incubated with 0.5 ml of assay buffer containing 5 μM of rhodamine 123 for 60 min. Then, the solution was removed and the cells were washed three times with ice-cold phosphate-buffered saline and solubilized in 1 M NaOH (0.2 ml). The solution was neutralized with 1 M HCl (0.2 ml) and the rhodamine 123 content was determined using a fluorescence multiwell plate reader (Ex(λ) 485 nm; Em(λ) 530 nm, CytoFluor Series 4000). The cellular protein was measured by the method of Bradford (1976).

2.7. Electrochemical monitoring of NO

Direct and continuous electrochemical measurement of NO was performed with a three-electrode potentiostatic EMS-100 system (BIO-LOGIC, Grenoble, France) as previously described (Ikesue et al., 2000, Trevin et al., 1998). In brief, confluent MBEC4 cells or rat astrocytes in a 2.5 cm^2 dish (BD FALCON™, BD Biosciences, NJ, USA) were washed three times with Mg^{2+}-free Krebs–Ringer solution (143.0 mM NaCl, 4.7 mM KCl, 2.5 mM $CaCl_2$, 1.0 mM NaH_2PO_4 and 11.0 mM D-glucose, pH 7.4). The dish was placed on the stage of an inverted microscope (ECLIPSE TE300, Nikon, Tokyo, Japan) mounted with a NO monitoring system. The NO-biosensor (ASTEC, Fukuoka, Japan) was positioned about 10 μm above the cell surface. Ten minutes after treatment with L-arginine (1 mM), histamine or phenylephrine in a volume of 10 μl was added to the cells in 1 ml of Mg^{2+}-free Krebs–Ringer solution with a transient mixing step to give the final concentration indicated. The level of production of NO in MBEC4 cells or rat astrocytes was monitored for a 15-min period after the addition of histamine or phenylephrine. Cyclosporine was added 20 min before treatment with L-arginine.

2.8. Assessment of cell viability

The effect of cyclosporine on the viability of cells in the MBEC4 monolayer, C6 coculture and rat astrocyte coculture systems was assessed using a WST-8 assay (Cell Counting Kit-8, DOJINDO, Kumamoto, Japan). A highly water-soluble formazan dye (WST-8), reduced by mitochondrial dehydrogenase, was measured by determining the absorbance of each sample with a 450 nm test wavelength and a 700 nm reference wavelength using a microplate reader (Opsys MR, DYNEX technologies, Chantilly, VA, USA).

2.9. Measurement of NO Production using NO-specific dye

An accumulation of NO production during a 12 h period was assessed using a NO-specific fluorescent dye, 4,5-diaminofluorescein diacetate (DAF-2 DA, Sigma) (Nakatsubo et al., 1998). MBEC4 and C6 cells were seeded on wells of the 24-well culture plate. Cells were

incubated with DAF-2 DA at a final concentration of 10 μM for 1 h at 37 °C and then rinsed three times with serum-free medium. Cells containing DAF2 DA were exposed to cyclosporine (1–5 μM) for 12 h and they were washed three times with assay buffer (143 mM NaCl, 4.7 mM KCl, 1.3 mM $CaCl_2$, 1.2 mM $MgCl_2$, 1.0 mM NaH_2PO_4, 10 mM HEPES, and 11 mM D-glucose, pH 7.4). The fluorescence was measured using a fluorescence multiwell plate reader (Ex(λ) 485 nm; Em(λ) 530 nm, CytoFluor Series 4000). Then, cells were solubilized with 250 μl of 1 M NaOH. Aliquots of the cell solution were removed for protein assay according to the method of Bradford using a Bio-Rad protein assay kit (Bio-Rad Laboratories, Hercules, CA) (Bradford, 1976). Data for each experiment were normalized to the cellular protein.

2.10. Statistical analysis

The values are expressed as the means±S.E.M. Statistical analysis was performed using Student's *t*-test. One way and two way analyses of variance (ANOVAs) followed by Tukey–Kramer's tests were applied to multiple comparisons. The differences between means were considered to be significant when *P* values were less than 0.05.

3. Results

3.1. Permeability and P-glycoprotein function of MBEC4 cells in MBEC4 monolayer, C6 coculture and rat astrocyte coculture systems

After MBEC4 cells were cultured for 3 days, the basal permeability and P-glycoprotein efflux pump of MBEC4 cells were evaluated in three in vitro blood–brain barrier models (Fig. 1). The permeability coefficient of Na-F for MBEC4 cells was increased by 57.6% in the C6 coculture and reduced by 45.6% in the rat astrocyte coculture, when compared to that in the MBEC4 monolayer (Fig. 1A). The accumulation of rhodamine 123 in MBEC4 cells was significantly increased by 16.8% in the C6 coculture and significantly reduced by 17.9% in the rat astrocyte coculture relative to the MBEC4 monolayer (Fig. 1B).

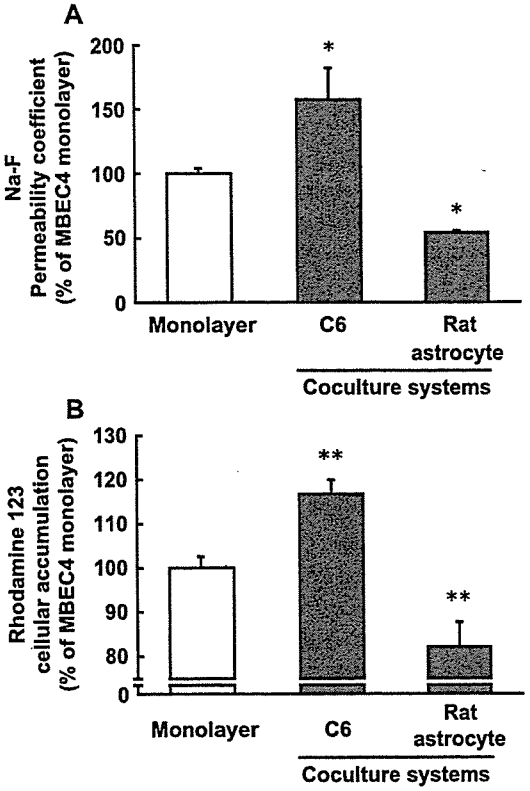

Fig. 1. Permeability and P-glycoprotein function of MBEC4 cells in MBEC4 monolayer, C6 coculture and rat astrocyte coculture systems. (A) MBEC4 permeability coefficients of Na-F. Results are expressed as % of the MBEC4 monolayer ($1.88\pm0.10\times10^{-4}$ cm/min). Values are the means± S.E.M. (n=3–7). *P<0.05, significant difference from MBEC4 monolayer. (B) Rhodamine 123 accumulation in MBEC4 cells. Results are expressed as % of the MBEC4 monolayer (2.19±0.16 nmol/mg protein). Values are the means±S.E.M. (n=4–17). **P<0.01, significant difference from MBEC4 monolayer.

3.2. Effect of cyclosporine on permeability and P-glycoprotein function of MBEC4 cells in MBEC4 monolayer, C6 coculture and rat astrocyte coculture systems

As shown in Figs. 2 and 3, the exposure to cyclosporine (1–5 μM) for 12 h dose-dependently increased the permeability of Na-F and the cellular accumulation of rhodamine 123 in the MBEC4 monolayer and C6 coculture. The Na-F permeability and the rhodamine 123 accumulation of MBEC4 cells in the rat astrocyte coculture were increased to 127.7±7.2% and 126.7±3.0% of vehicle by 5 μM cyclosporine. These adverse effects of cyclosporine in the presence of C6 cells and astrocytes were two- to threefold more potent than the effects in the MBEC4 monolayer.

The WST-8 assay showed that cyclosporine at the highest concentration tested (5 μM) had no effect on cell viability in any of the three culture systems (MBEC4 monolayer: 98.2±1.00, C6 coculture: 101.2±1.79, rat astrocyte coculture: 103.9±7.5% of the corresponding vehicle).

3.3. Effect of cyclosporine on stimulation-evoked NO production and spontaneous NO production in MBEC4 cells, rat astrocytes and C6 cells

Cyclosporine alone at concentrations less than 5 μM failed to stimulate NO production to a detectable level (Fig. 4). In the absence of cyclosporine, histamine (100 μM) and phenylephrine (1 μM) produced small amounts of NO in MBEC4 cells and rat astrocytes (9.27±0.69 and 0.32±0.036 μM), respectively (Fig. 4). Cyclosporine (1, 2 and 5 μM) dose-dependently increased histamine (100 μM)- and phenylephrine (1 μM)-evoked NO production in MBEC4 cells and astrocytes, respectively (Fig. 4). The increases induced by 5 μM cyclosporine reached

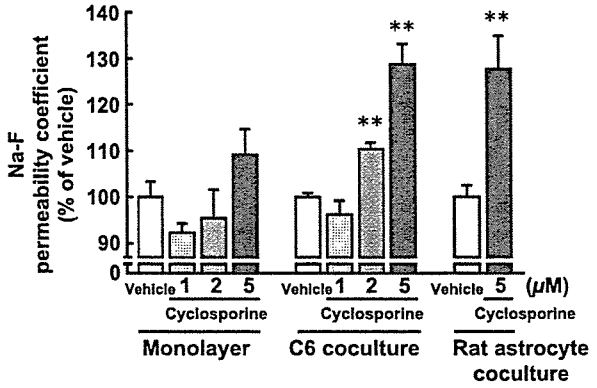

Fig. 2. Effect of cyclosporine on MBEC4 permeability of Na-F in MBEC4 monolayer, C6 coculture and rat astrocyte coculture systems. Transport experiments were performed after 12 h of exposure to cyclosporine. Results are expressed as % of each corresponding vehicle (monolayer; $2.35\pm0.24\times10^{-4}$ cm/min, C6 coculture; $2.34\pm0.25\times10^{-4}$ cm/min, rat astrocyte coculture; $1.16\pm0.03\times10^{-4}$ cm/min). Values are the means± S.E.M. (n=3–24). **P<0.01, significant difference from each corresponding vehicle.

174.1±7.7% and 198.2±15.0% of vehicle in MBEC4 cells and astrocytes, respectively.

When total amounts of NO production during a 12 h period was measured using a NO-specific fluorescent dye, an exposure of cyclosporine (5 μM) for 12 h significantly increased spontaneous (basal) NO production by 70 and 190% in MBEC4 and C6 cells, respectively (Fig. 5).

3.4. Effect of NO synthase inhibitor on cyclosporine-increased permeability of Na-F and accumulation of rhodamine 123 in MBEC4 monolayer and rat astrocyte coculture systems

L-NMMA (1 mM) (a NOS inhibitor) alone had no effect on the permeability of Na-F and the accumulation of rhodamine 123 in the MBEC4 monolayer and C6 coculture.

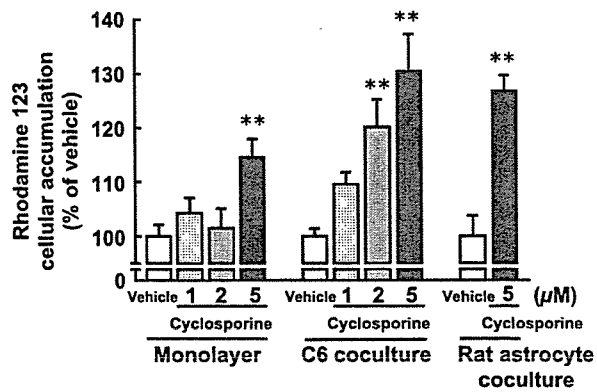

Fig. 3. Effect of cyclosporine on rhodamine 123 accumulation in MBEC4 cells of the MBEC4 monolayer, C6 coculture and rat astrocyte coculture systems. P-glycoprotein function was evaluated after 12 h of exposure to cyclosporine. Results are expressed as % of each corresponding vehicle (monolayer; 3.50±0.56 nmol/mg protein, C6 coculture; 3.79±0.47 nmol/mg protein, rat astrocyte coculture; 0.85±0.04 nmol/mg protein). Values are the means±S.E.M. (n=4–20). **P<0.01, significant difference from each corresponding vehicle.

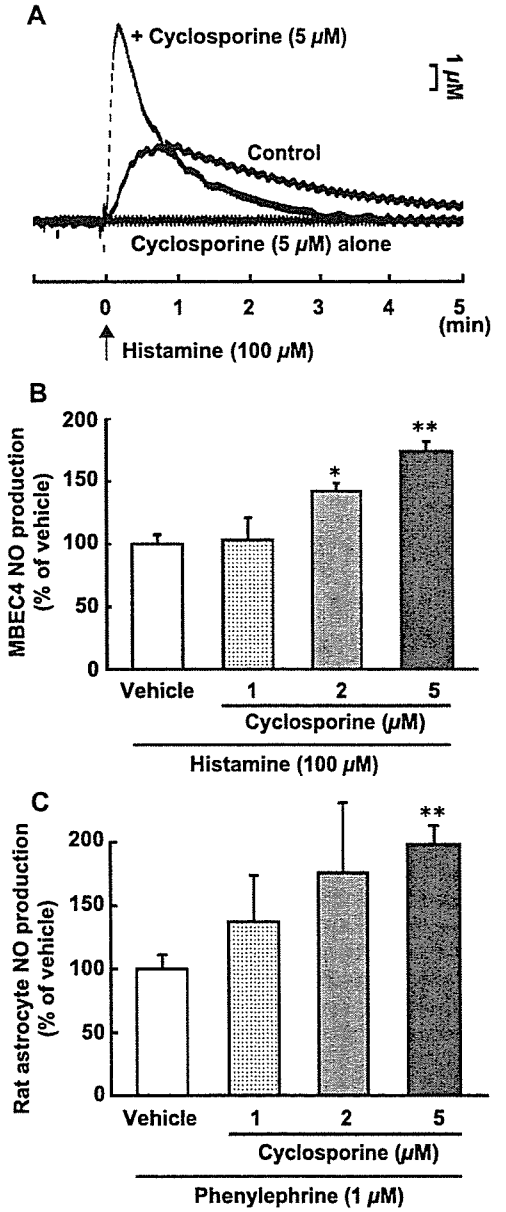

Fig. 4. Effect of cyclosporine on stimulations-evoked NO production. (A) Representative differential pulse amperogram obtained using NO biosensor shows NO production evoked by histamine (100 μM) in the absence (Control, middle trace) and presence of cyclosporine (5 μM) (+cyclosporine, top trace) in MBEC4 cells. The effect of cyclosporine (5 μM) alone on NO production was indicated in the bottom trace. (B) Concentration-dependent facilitatory effect of cyclosporine on histamine-evoked NO production in MBEC4 monolayer. Results are expressed as % of histamine (100 μM)-evoked NO production (vehicle; 9.27±0.69 μM). Values are the means± S.E.M. (n=3). *P<0.05 and **P<0.01, significant differences from vehicle. (C) Concentration-dependent facilitatory effect of cyclosporine on phenylephrine-evoked NO production in rat astrocyte coculture system. Results are expressed as % of phenylephrine (1 μM)-evoked NO production (vehicle; 0.32±0.036 μM). Values are the means±S.E.M. (n=4–7). *P<0.05 and **P<0.01, significant differences from vehicle.

Cyclosporine (5 μM)-increased permeability of Na-F and accumulation of rhodamine 123 in MBEC4 cells were significantly decreased to 114.3±5.9% and 112.6±3.7% of

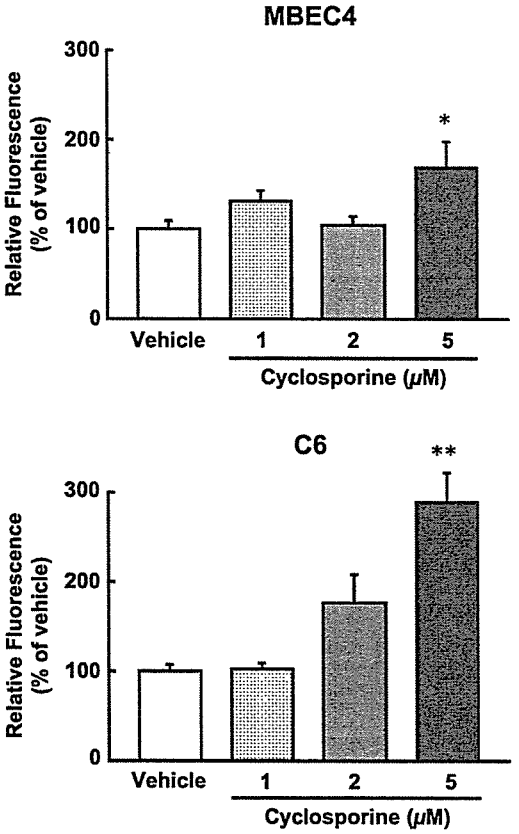

Fig. 5. Effect of cyclosporine on spontaneous NO production in MBEC4 and C6 cells. Cells were loaded with a NO-specific fluorescent dye (DAF-2 DA) and then treated with 1–5 μM cyclosporine for 12 h. The fluorescence intensity of DAF-2 DA was increased by NO produced by cells and this was normalized to the cellular protein. Relative fluorescence is expressed as the ratio (%) to the control value obtained in the absence of cyclosporine (vehicle). Values are the means±S.E.M. (n=8). *P<0.05, significant differences from vehicle.

vehicle, respectively, by 1 mM L-NMMA in the C6 coculture (Fig. 6). In contrast, L-NMMA (1 mM) produced a slight inhibition of the permeability of Na-F and the accumulation of rhodamine 123 induced by Cyclosporine (5 μM) in the MBEC4 monolayer (Fig. 6).

4. Discussion

We made three types of the in vitro blood–brain barrier models; MBEC4 monolayer, C6 coculture, and rat astrocyte coculture systems. MBEC4 cells alone show the highly specialized characteristics of brain microvascular endothelial cells including the integration of tight junctions and expression of P-glycoprotein (Tatsuta et al., 1992, 1994). Astrocytes, a cellular component of the blood–brain barrier, induce and maintain the functioning of the blood–brain barrier through cell-to-cell contact and the secretion of soluble factors (Rubin and Staddon, 1999). The barrier function in these models was evaluated based on the permeability of Na-F and the P-glycoprotein efflux pump of MBEC4 cells. Na-F was used as a marker of permeability through the paracellular route. The permeability and the accumulation of rhodamine 123 in MBEC4 cells were markedly decreased in the presence of rat astrocytes (Fig. 1). These findings suggest that astrocytes participate in tightening the intercellular junctions and facilitating P-glycoprotein function of brain endothelial cells. A positive role for astrocytes in the expression and maintenance of endothelial tight junctions has been documented (Dehouck et al., 1992; Gaillard et al., 2001; Isobe et al., 1996; Rauh et al., 1992; Hayashi et al., 1997), although there are few reports concerning astrocyte-enhanced P-glycoprotein function. The C6 cell line, which originated from rat glioma cells, is commonly used as an experimental model of astrocytes due to convenient handling (Zhang et al., 2004). The barrier function of MBEC4 cells was speculated to be

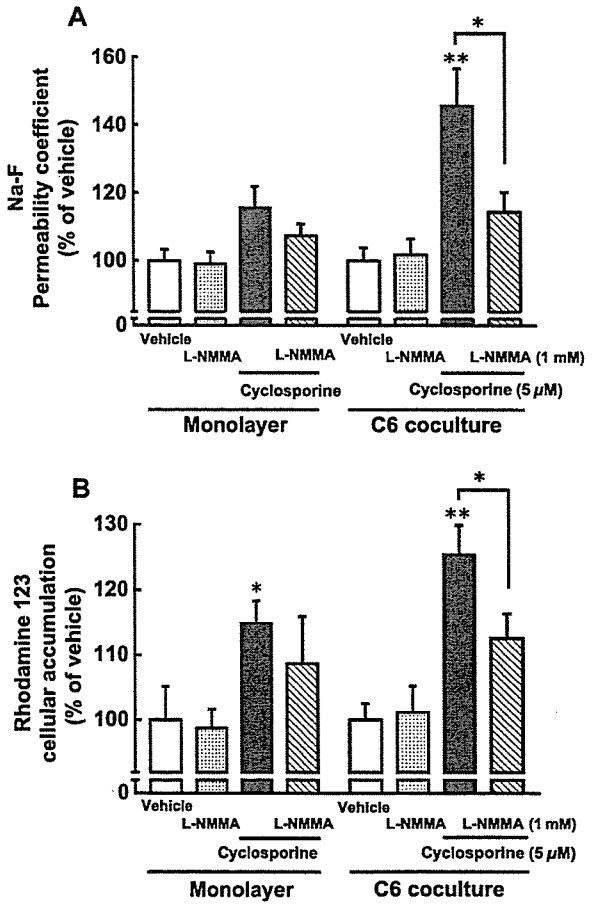

Fig. 6. Effect of NO synthase inhibitor (L-NMMA) on cyclosporine-increased MBEC4 permeability of Na-F (A), and rhodamine 123 accumulation in MBEC4 cells (B) in MBEC4 monolayer and C6 coculture system. (A) Results are expressed as % of each corresponding vehicle (monolayer; $1.73\pm0.10\times10^{-4}$ cm/min, C6 coculture; $2.95\pm0.55\times10^{-4}$ cm/min). Values are the means±S.E.M. (n=7–11). *P<0.05, **P<0.01, significant difference from each corresponding vehicle. (B) Results are expressed as % of each corresponding vehicle (monolayer; 14.2±3.94 nmol/mg protein, C6 coculture; 9.05±2.00 nmol/mg protein). Values are the means±S.E.M. (n=7–12). *P<0.05, **P<0.01, significant differences from each corresponding vehicle.

enhanced by the C6 cells similar the rat astrocyte coculture. However, the present findings indicated hyperpermeability of Na-F and reduced P-glycoprotein function in the C6 coculture. These results may be due to neoplastic changes in the glial characteristics. The precise mechanism by which C6 cells affect the barrier function of MBEC4 cells is now under investigation. There were no apparent differences in the endothelial cell response to cyclosporine between the C6 coculture and rat astrocyte coculture (Figs. 2 and 3). This confirms that the C6 coculture model is suitable for pharmacological research.

Cyclosporine-induced neurotoxicity including tremors, convulsions and encephalopathy occurred frequently in patients with high blood concentrations of cyclosporine, although these concentrations were within the therapeutic range (Gijtenbeek et al., 1999). The maximal blood concentrations of cyclosporine in patients with renal or liver transplantation are known to be in the range varying from 1 to 1.5 μM (Kahan et al., 1995; Keown and Niese, 1998; Grant et al., 1999). Therefore, the concentrations (1–5 μM) of cyclosporine used in the present study are less than three- to fivefold level of the maximal concentrations in patients. Cyclosporine (5 μM) significantly increased the permeability of Na-F and the accumulation of rhodamine 123 in the MBEC4 monolayer. These effects were potentiated markedly in the coculture with C6 cells or rat astrocytes (Figs. 2 and 3). Then, we substituted C6 cells for the primary culture of rat astrocytes to save the experimental animals, costs and labor in the subsequent pharmacological study. The presence of C6 cells increased by two- to threefold the facilitatory and inhibitory effects of cyclosporine (1–5 μM) on the paracellular permeability and P-glycoprotein activity of the MBEC4 monolayer, respectively. These effects were not due to the direct cytotoxicity of cyclosporine. These findings indicated that cyclosporine reduces the barrier function of brain endothelial cells to penetrate into the brain, leading to further aggravation of the blood–brain barrier function by interacting with astrocytes.

A 12-h exposure of cyclosporine (5 μM) in the same schedule as the blood–brain barrier function test significantly increased the accumulation of spontaneous NO production during a 12-h period, when measured using a NO-specific fluorescent dye (Fig. 5). A direct electrochemical NO monitoring failed to detect cyclosporine-increased basal NO production (Fig. 4). This monitoring method is capable of detecting a rapid NO production in response to the stimulation as a sharp current–time curve, even if amounts of NO production are small. However, NO biosensor is relatively difficult to detect a slow NO production with a low peak and a long-lasting plateau phase, even if total amounts during a long period is large. Cyclosporine dose-dependently enhanced histamine- and phenylephrine-evoked NO production in MBEC4 cells and rat astrocytes, respectively (Fig. 4). Cyclosporine exerts pharmacological effects by binding to cyclophilin (peptidyl-propyl isomerase), a highly basic and abundant cytosolic protein (Marks, 1996). This cyclosporine/cyclophilin complex inhibits calcineurin, a serine–threonine phosphatase 2B, thereby blocking its phosphatase activity (Marks, 1996; Yakel, 1997). Calcineurin regulates the activity of ion channels and neurotransmitter release. Calcineurin anchored to the inositol 1,4,5-triphosphate (IP_3) receptor via FKBP12, a FK506-binding protein, regulates the phosphorylation status of the receptor, resulting in a dynamic Ca^{2+}-sensitive regulation of IP_3-mediated Ca^{2+} flux (Cameron et al., 1997). In contrast with FKBP12, cyclophilin does not bind to the IP_3 receptor (Cameron et al., 1995). However, when rat cerebellar microsomes were treated with cyclosporine and cyclophilin, protein kinase C-induced IP_3 receptor phosphorylation and IP_3-stimulated Ca^{2+} flux were markedly increased (Cameron et al., 1995). This suggests that cyclosporine inhibits the dephosphorylation of the IP_3 receptor to maintain a leaky IP_3 receptor channel that was phosphorylated by serine–threonine protein kinases such as protein kinase C. Although the IP_3 receptor becomes leaky, cyclosporine alone appears incapable of elevating $[Ca^{2+}]_{IN}$ over the threshold for activation of the constitutive NO synthase. This may explain the present findings that cyclosporine alone failed to raise NO production above the detection limit of the NO biosensor, while the histamine and phenylephrine-evoked NO production in MBEC4 and C6 cells, respectively, was markedly facilitated by cyclosporine. Histamine and phenylephrine activate phospholipase C through the H_1 receptor and α_1-adrenoceptor, respectively, to generate IP_3 (Lum and Malik, 1994; Daum et al., 1983) and stimulate the leaky Ca^{2+} channel (phosphorylation status of IP_3 receptor) maintained by cyclosporine. These events probably lead to the markedly higher level of $[Ca^{2+}]_{IN}$ than that induced by histamine and phenylephrine in MBEC4 cells and rat astrocytes, respectively. We previously reported that cyclosporine also enhanced α_1-adrenoceptor-mediated NO production in C6 cells (Ikesue et al., 2000). In the brain, various biological substances including noradrenaline, glutamate, histamine and endothelin stimulate G protein-coupled receptors that have a common intracellular signaling pathway (IP_3/diacylglycerol) in astrocytes (Verkhratsky and Kettenmann, 1996). This endogenous stimulator-evoked NO production is highly likely to be augmented by cyclosporine via a mechanism similar to that proposed here. In fact, our in vivo microdialysis experiment showed that an intraperitoneal injection of cyclosporine significantly increased NO production in the rat dorsal hippocampus (Fujisaki et al., 2002).

The present study demonstrated that cyclosporine impaired the barrier function of brain endothelial cells and this effect was remarkably potentiated by co-culturing MBEC4 cells with C6 cells or rat astrocytes. A NO synthase inhibitor, L-NMMA at a concentration of 1 mM showed no effect on the Na-F permeability and the rhodamine 123 accumulation of MBEC4 cells in both culture systems (Fig. 6), suggesting that L-NMMA (1 mM)

has not nonspecific effect on the basal blood–brain barrier functions of MBEC4 cells. L-NMMA (1 mM) significantly blocked the cyclosporine-induced increase in the permeability of Na-F and accumulation of rhodamine 123 in the C6 coculture. This protective effect was moderate in the MBEC4 monolayer (Fig. 6). These findings suggest that cyclosporine-enhanced NO production in astrocytes largely contributes to an impairment of the blood–brain barrier. This notion is supported by our previous findings that NO lowered the function of tight junctions and P-glycoprotein at the blood–brain barrier (Yamauchi et al., in press). The mechanisms by which NO donors increased vascular endothelial permeability involved an increase in the level of cGMP (Gimeno et al., 1998) or the formation of peroxynitrite (Menconi et al., 1998). These substances conceivably influence intrinsic tight junction proteins and the associated actin cytoskeleton through a direct or second signaling pathway (Burgstahler and Nathanson, 1995; Liu and Sundqvist, 1997). It is, therefore, likely that cyclosporine passes through the slightly impaired barrier of brain endothelial cells and then acts on astrocytes to enhance NO production, leading to further aggravation of the blood–brain barrier impairment.

In conclusion, cyclosporine accelerated stimulation-evoked NO production in brain endothelial and astroglial cells. This enhanced production of NO that interacts with each cellular component of the blood–brain barrier is involved in the sequential process of blood–brain barrier functional impairment induced by cyclosporine.

Acknowledgements

This work was supported, in part, by Grants-in-Aid for Scientific Research ((B)(2) 14370789) and ((C)(2) 15590475) from JSPS, Japan, by a Grant-in-Aid for Exploratory Research (16659138) from MEXT, Japan and by funds (No.: 031001) from the Central Research Institute of Fukuoka University.

References

Bradford, M.M., 1976. A rapid and sensitive method for the quantitation of microgram quantities of protein utilizing the principle of protein-dye binding. Anal. Biochem. 72, 248–254.

Burgstahlar, A.D., Nathanson, M.H., 1995. NO modulates the apicolateral cytoskeleton of isolated hepatocytes by a PKC-dependent, cGMP-independent mechanism. Am. J. Physiol. 276, G789–G799.

Cameron, A.M., Steiner, J.P., Roskams, A.J., Ali, S.M., Ronnett, G.V., Snyder, S.H., 1995. Calcineurin associated with the inositol 1,4,5-trisphosphate receptor-FKBP12 complex modulates Ca^{2+} flux. Cell 83, 463–472.

Cameron, A.M., Nucifora, F.C., Fung, E.T., Livingston, D.J., Aldape, R.A., Ross, C.A., Snyder, S.H., 1997. FKBP12 binds the inositol 1,4,5-trisphosphate receptor at leucine-proline (1400–1401) and anchors calcineurin to this FK506-like domain. J. Biol. Chem. 272, 27582–27588.

Daum, P.R., Downes, C.P., Young, J.M., 1983. Histamine-induced inositol phospholipids breakdown mirrors H_1-receptor density in brain. Eur. J. Pharmacol. 87, 497–498.

Dehouck, M.-P., Jolliet-Riant, P., Brée, F., Fruchart, J.-C., Cecchelli, R., Tillement, J.-P., 1992. Drug transfer across the blood–brain barrier: correlation between in vitro and in vivo models. J. Neurochem. 58, 1790–1797.

Dohgu, S., Kataoka, Y., Ikesue, H., Naito, M., Tsuruo, T., Oishi, R., Sawada, Y., 2000. Involvement of glial cells in cyclosporine-increased permeability of brain endothelial cells. Cell. Mol. Neurobiol. 20, 781–786.

Fontaine, M., Elmquist, W.F., Miller, D.W., 1996. Use of rhodamine 123 to examine the functional activity of P-glycoprotein in primary cultured brain microvessel endothelial cell monolayers. Life Sci. 59, 1521–1531.

Fujisaki, Y., Yamauchi, A., Dohgu, S., Sunada, K., Yamaguchi, C., Oishi, R., Kataoka, Y., 2002. Cyclosporine A-increased nitric oxide production in the rat dorsal hippocampus mediates convulsions. Life Sci. 72, 549–556.

Gaillard, P.J., Voorwinden, L.H., Nielsen, J.L., Ivanov, A., Atsumi, R., Engman, H., Ringbom, C., de Boer, A.G., Breimer, D.D., 2001. Establishment and functional characterization of an in vitro model of the blood–brain barrier, comprising a co-culture of brain capillary endothelial cells and astrocyte. Eur. J. Pharm. Sci. 12, 215–222.

Gijtenbeek, J.M.M., van den Bent, M.J., Vecht, Ch.J., 1999. Cyclosporine neurotoxicity: a review. J. Neurol. 246, 339–346.

Gimeno, G., Carpentier, P.H., Desquand-Billiald, S., Hanf, R., Finet, M., 1998. L-Arginine and *N*G-nitro-L-arginine methyl ester cause macromolecular extravasation in the microcirculation of awake hamsters. Eur. J. Pharmacol. 346, 275–282.

Grant, D., Kneteman, N., Tchervenkov, J., Roy, A., Murphy, G., Tan, A., Hendricks, L., Guilbault, N., Levy, G., 1999. Peak cyclosporine levels (Cmax) correlate with freedom from liver graft rejection: results of a prospective, randomized comparison of neoral and sandimmune for liver transplantation (NOF-8). Transplantation 67, 1133–1137.

Hayashi, Y., Nomura, M., Yamagishi, S., Harada, S., Yamashita, J., Yamamoto, H., 1997. Induction of various blood–brain barrier properties in non-neural endothelial cells by close apposition to co-cultured astrocytes. Glia 19, 13–26.

Ikesue, H., Kataoka, Y., Kawachi, R., Dohgu, S., Shuto, H., Oishi, R., 2000. Cyclosporine enhances (α_1-adrenoceptor-mediated nitric oxide production in C6 glioma cells. Eur. J. Pharmacol. 407, 221–226.

Isobe, I., Watanabe, T., Yotsuyanagi, T., Hazemoto, N., Yamagata, K., Ueki, T., Nakanishi, K., Asai, K., Kato, T., 1996. Astrocytic contributions to blood–brain barrier (BBB) formation by endothelial cells: a possible use of aortic endothelial cell for in vitro model. Neurochem. Int. 28, 523–533.

Kahan, B.D., 1989. Cyclosporine. N. Engl. J. Med. 321, 1725–1738.

Kahan, B.D., Dunn, J., Fitts, C., Van Buren, D., Wombolt, D., Pollak, R., Carson, R., Alexander, J.W., Choc, M., Wong, R., 1995. Reduced inter- and intrasubject variability in cyclosporine pharmacokinetics in renal transplant recipients treated with a microemulsion formulation in conjunction with fasting, low-fat meals, or high-fat meals. Transplantation 59, 505–511.

Keown, P., Niese, D., 1998. Cyclosporine microemulsion increases drug exposure and reduces acute rejection without incremental toxicity in de novo renal transplantation. International Sandimmun Neoral Study Group. Kidney Int. 54, 938–944.

Kochi, S., Takanaga, H., Matsuo, H., Naito, M., Tsuruo, T., Sawada, Y., 1999. Effect of cyclosporine A or tacrolimus on the function of blood–brain barrier cells. Eur. J. Pharmacol. 372, 287–295.

Kochi, S., Takanaga, H., Matsuo, H., Ohtani, H., Naito, M., Tsuruo, T., Sawada, Y., 2000. Induction of apoptosis in mouse brain capillary endothelial cells by cyclosporin A and tacrolimus. Life Sci. 66, 2255–2260.

Liu, S.M., Sundqvist, T., 1997. Nitric oxide and cGMP regulate endothelial permeability and F-actin distribution in hydrogen peroxide-treated endothelial cells. Exp. Cell Res. 235, 238–244.

Lum, H., Malik, A.B., 1994. Regulation of vascular endothelial barrier function. Am. J. Physiol. 267, L223–L241.

Marks, A.R., 1996. Cellular functions of immunophilins. Physiol. Rev. 76, 631–649.

McCarthy, K.D., de Vellis, J., 1980. Preparation of separate astroglial and oligodendroglial cell cultures from rat cerebral tissue. J. Cell Biol. 85, 890–902.

Menconi, M.J., Unno, N., Smith, M., Aguirre, D.E., Fink, M.P., 1998. Nitric oxide donor-induced hyperpermeability of cultured intestinal epithelial monolayers: role of superoxide radical, hydroxyl radical, and peroxynitrite. Biochem. Biophys. Acta 1425, 189–203.

Nakatsubo, N., Kojima, H., Kikuchi, K., Nagoshi, H., Hirata, Y., Maeda, D., Imai, Y., Irimura, T., Nagano, T., 1998. Direct evidence of nitric oxide production from bovine aortic endothelial cells using new fluorescence indicators: diaminofluoresceins. FEBS Lett. 427, 263–266.

Partridge, W.M., 1999. Blood–brain barrier biology and methodology. J. Neurovirology 5, 556–569.

Pirsch, J.D., Miller, J., Deierhoi, M.H., Vincenti, F., Filo, R.S., 1997. A comparison of tacrolimus (FK506) and cyclosporine for immunosuppression after cadaveric renal transplantation. FK506 kidney transplant study group.. Transplantation 63, 977–983.

Rauh, J., Meyer, J., Beuckmann, C., Galla, H.-J., 1992. Development of an in vitro cell culture system to mimic the blood–brain barrier. Prog. Brain Res. 91, 117–121.

Rubin, L.L., Staddon, J.M., 1999. The cell biology of the blood–brain barrier. Annu. Rev. Neurosci. 22, 11–28.

Sastradipura, D.F., Nakanishi, H., Tsukuba, T., Nishishita, K., Sakai, H., Kato, Y., Gotow, T., Uchiyama, Y., Yamamoto, K., 1998. Identification of cellular compartments involved in processing of cathepsin E in primary cultures of rat microglia. J. Neurochem. 70, 2045–2056.

Schinkel, A.H., 1999. P-glycoprotein, a gatekeeper in the blood–brain barrier. Adv. Drug Deliv. Rev. 5, 179–194.

Shuto, H., Kataoka, Y., Kanaya, A., Matsunaga, K., Sueyasu, M., Oishi, R., 1998. Enhancement of serotonergic neural activity contributes to cyclosporine-induced tremors in mice. Eur. J. Pharmacol. 341, 33–37.

Shuto, H., Kataoka, Y., Fujisaki, K., Nakao, T., Sueyasu, M., Miura, I., Watanabe, Y., Fujiwara, M., Oishi, R., 1999. Inhibition of GABA system involved in cyclosporine-induced convulsions. Life Sci. 65, 879–887.

Tatsuta, T., Naito, M., Oh-hara, T., Sugawara, I., Tsuruo, T., 1992. Functional involvement of P-glycoprotein in blood–brain barrier. J. Biol. Chem. 267, 20383–20391.

Tatsuta, T., Naito, M., Mikami, K., Tsuruo, T., 1994. Enhanced expression by the brain matrix of P-glycoprotein in brain capillary endothelial cells. Cell Growth Differ. 5, 1145–1152.

Terasaki, T., Ohtsuki, S., Hori, S., Takanaga, H., Nakashima, E., Hosoya, K., 2003. New approaches to in vitro models of blood–brain barrier drug transport. Drug Discov. Today 8, 944–954.

Trevin, S., Kataoka, Y., Kawachi, R., Shuto, H., Kumakura, K., Oishi, R., 1998. Direct and continuous electrochemical measurement of noradrenaline-induced nitric oxide production in C6 glioma cells. Cell. Mol. Neurobiol. 18, 453–458.

The U.S. Multicenter FK506 Liver Study Group, 1994. A comparison of tacrolims (FK 506) and cyclosporine for immunosuprresion in liver transplantation. N. Engl. J. Med. 331, 1110–1115.

Verkhratsky, A., Kettenmann, H., 1996. Calciun signaling in gilal cells. Trends Neurosci. 19, 346–352.

Yakel, J.L., 1997. Calcineurin regulation of synaptic function: from ion channels to transmitter release and gene transcription. Trends Pharmacol. Sci. 18, 124–134.

Yamauchi, A., Donghu, S., Naito, M., Tsuruo, T., Sawada, Y., Kai, M., Kataoka, Y. Nitric oxide lowers the function of tight junction and P-glycoprotein at the blood-brain barrier. Cell. Mol. Neurobiol. (in press).

Zhang, X.-D., Morishima, S., Ando-Akatsuka, Y., Takahashi, N., Nabekura, T., Inoue, H., Shimizu, T., Okada, Y., 2004. Expression of novel isoforms of the ClC-1 chloride channel in astrocytic glial cells in vitro. Glia 47, 46–57.

Cellular and Molecular Neurobiology, Vol. 24, No. 2, April 2004 (© 2004)

Uptake and Efflux of Quinacrine, a Candidate for the Treatment of Prion Diseases, at the Blood-Brain Barrier

Shinya Dohgu,[1,2] Atsushi Yamauchi,[2] Fuyuko Takata,[2] Yasufumi Sawada,[1] Shun Higuchi,[1] Mikihiko Naito,[3] Takashi Tsuruo,[3] Susumu Shirabe,[4] Masami Niwa,[4] Shigeru Katamine,[4] and Yasufumi Kataoka[2,5]

Received April 7, 2003; accepted May 22, 2003

SUMMARY

1. A clinical trial of quinacrine in patients with Creutzfeldt–Jakob disease is now in progress. The permeability of drugs through the blood–brain barrier (BBB) is a determinant of their therapeutic efficacy for prion diseases. The mechanism of quinacrine transport across the BBB was investigated using mouse brain endothelial cells (MBEC4).

2. The permeability of quinacrine through MBEC4 cells was lower than that of sodium fluorescein, a BBB-impermeable marker. The basolateral-to-apical transport of quinacrine was greater than its apical-to-basolateral transport. In the presence of P-glycoprotein (P-gp) inhibitor, cyclosporine or verapamil, the apical-to-basolateral transport of quinacrine increased. The uptake of quinacrine by MBEC4 cells was enhanced in the presence of cyclosporine or verapamil.

3. Quinacrine uptake was highly concentrative, this event being carried out by a saturable and carrier-mediated system with an apparent K_m of 52.1 μM. Quinacrine uptake was insensitive to Na^+-depletion and changes in the membrane potential and sensitive to changes in pH. This uptake was decreased by tetraethylammonium and cimetidine, a substrate and an inhibitor of organic cation transporters, respectively.

4. These findings suggest that quinacrine transport at the BBB is mediated by the efflux system (P-gp) and the influx system (organic cation transporter-like machinery).

KEY WORDS: quinacrine; blood–brain barrier; mouse brain endothelial cells; P-glycoprotein; organic cation transporter; Creutzfeldt–Jakob disease.

INTRODUCTION

Prion diseases including Creutzfeldt–Jakob disease (CJD) are progressive, fatal neurodegenerative diseases induced by conformational changes in prion protein (PrP) in

[1] Department of Medico-Pharmaceutical Sciences, Graduate School of Pharmaceutical Sciences, Kyushu University, Fukuoka, Japan.

[2] Department of Pharmaceutical Care and Health Sciences, Faculty of Pharmaceutical Sciences, Fukuoka University, Fukuoka, Japan.

[3] Institute of Molecular and Cellular Biosciences, University of Tokyo, Tokyo, Japan.

[4] Nagasaki University Graduate School of Biomedical Sciences, Nagasaki, Japan.

[5] To whom correspondence should be addressed at Department of Pharmaceutical Care and Health Sciences, Faculty of Pharmaceutical Sciences, Fukuoka University, 8-19-1 Nanakuma, Jonan-ku, Fukuoka 814-0180, Japan; e-mail: ykataoka@cis.fukuoka-u.ac.jp.

0272-4340/04/0400-0205/0

the central nervous system. It has been reported that quinacrine, an antimalarial drug, could rapidly eradicate production of the disease-associated and protease-resistant isoform of the prion protein (PrP^{SC}) in vitro (Korth *et al.*, 2001). A clinical trial of quinacrine has started at the Department of Neurology, Faculty of Medicine, Fukuoka University and the Department of Neurology, Faculty of Medicine, Nagasaki University. A transient improvement was observed in CJD patients (Follette, 2003).

The members of organic cation transporter (OCT) family include OCT1 (Grundemann *et al.*, 1994), OCT2 (Okuda *et al.*, 1996), OCT3 (Kekuda *et al.*, 1998), novel organic cation transporter (OCTN)1 (Tamai *et al.*, 1997), OCTN2 (Wu *et al.*, 1998), and OCTN3 (Tamai *et al.*, 2000). The tissue distribution patterns of the OCT family are dependent on the animal species. In the human and rat brain, OCT2 mRNA (Koepsell, 1998), OCTN1 mRNA (Tamai *et al.*, 1997; Wu *et al.*, 2000), and OCTN2 mRNA (Wu *et al.*, 1998, 1999) have been detected. OCTN1 and OCTN2 are expressed in the mouse brain (Tamai *et al.*, 2000). Immortalized rat brain endothelial cells (RBE4) express OCTN2 (Friedrich *et al.*, 2003). OCTN1 and OCTN2 are structurally much more closely related to each other than to OCT1, OCT2, and OCT3 (Wu *et al.*, 2000). Quinacrine is an organic cation and an organic base. The entry of organic cations such as choline into the brain occurs via transport systems present in the blood brain barrier (BBB) (Friedrich *et al.*, 2001; Sawada *et al.*, 1999). The transport of L-carnitine was mediated by OCTN2 in RBE4 cells (Friedrich *et al.*, 2003). Quinacrine inhibited tetraethylammonium (TEA) transport in MDCK cells expressing rat OCT2 (Sweet and Pritchard, 1999).

The BBB permeability of quinacrine is a determinant of its therapeutic efficacy for CJD. Quinacrine is known to pass through the BBB (Korth *et al.*, 2001), although the extent of quinacrine penetration into the brain and the mechanism involved in quinacrine transport across the BBB remain obscure. In this study, we investigated the properties of quinacrine transport into the brain using mouse brain capillary endothelial cells (MBEC4).

MATERIALS AND METHODS

Materials

Quinacrine dihydrochloride and sodium azide (NaN_3) were purchased from Tokyo Kasei Kogyo (Tokyo, Japan) and Kishida Kagaku (Osaka, Japan), respectively. N-Methylglucamine, 2,4-dinitrophenol (DNP), carbonyl cyanide *p*-(trifluoromethoxy) phenylhydrazone (FCCP), valinomycin, amiloride, tetraethylammonium (TEA), cimetidine, and verapamil were purchased from Sigma (St. Louis, MO). Cyclosporine was kindly supplied by Novartis (Basel, Switzerland). All other chemicals were commercial products of reagent grade.

Cell Culture

MBEC4 cells isolated from BALB/c mice brain cortices and immortalized by SV40-transformation (Tatsuta *et al.*, 1992) were cultured in Dulbecco's modified Eagle's medium (DMEM) (GIBCO BRL, Life Technologies, Grand Island, NY)

supplemented with 10% fetal bovine serum, 100 units/mL penicillin, and 100 μg/mL streptomycin in a humidified atmosphere of 5% CO_2/95% air at 37°C. For the transport experiments, MBEC4 cells (42,000 cells/cm^2) were plated into the collagen-coated polycarbonate membrane (1.0 cm^2, 3.0-μm pore size) of the Transwell^{TM} insert (12-well type) (Costar, MA). For the cellular uptake experiments, cells were seeded at a density of 21,000 cells/cm^2 on 4- or 24-well multi dishes (Nunc, Roskilde, Denmark). MBEC4 cells were cultured for 3 days and then used for the following experiments. MBEC4 cells show both general brain endothelial and specific BBB characteristics including the expression of P-glycoprotein (P-gp) (Tatsuta *et al.*, 1992, 1994).

Transcellular Transport of Quinacrine Across MBEC4 Cells

To initiate the transport experiments, the medium was removed and cells were washed three times with Krebs-Ringer buffer (118 mM NaCl, 4.7 mM KCl, 1.3 mM $CaCl_2$, 1.2 mM $MgSO_4$, 1.0 mM NaH_2PO_4, 25 mM $NaHCO_3$, 11 mM D-glucose, pH 7.4). Krebs-Ringer buffer was applied on the outside of the insert in the well (abluminal side) (1.5 mL) and the luminal side of the insert (0.5 mL). Krebs-Ringer buffer containing 50–200 μM quinacrine (MW 473) or 100 μM sodium fluorescein (Na-F) (MW 376), a paracellular transport marker, was loaded on the luminal or abluminal side of the insert. Samples (0.5 mL) were removed from the luminal or abluminal chamber at 10, 20, 30, and 60 min and immediately replaced with fresh Krebs-Ringer buffer. The quinacrine concentration in the samples was determined using a multiwell fluorometer (Ex(λ) 450 nm; Em(λ) 530 nm) (CytoFluor Series 4000, PerSeptive Biosystems, Framingham, MA). Aliquots (5 μL) from the samples were mixed with 200 μL of Krebs-Ringer buffer and then the concentration of Na-F was measured (Ex(λ) 485 nm; Em(λ) 530 nm). Permeability coefficient and clearance were calculated according to the method described by Dehouck *et al.* (1992). Clearance was expressed as μL of tracer diffusing from the luminal to the abluminal chambers and was calculated from the initial concentration of tracer in the luminal chamber and the final concentration of tracer in the abluminal chamber: *Clearance* (μL) = $[C]_A \times V_A/[C]_L$ where $[C]_L$ is the initial luminal tracer concentration, $[C]_A$ is the abluminal tracer concentration, and V_A is the volume of the abluminal chamber. During the 60-min period of the experiment, the clearance volume increased linearly with time. The average volume cleared was plotted versus time, and the slope was estimated by linear regression analysis. The slope of clearance curves for the MBEC4 monolayer was denoted PS_{app}, where PS is the permeability $\times$ surface area product (in μL per min). The slope of the clearance curve with the control membrane was denoted $PS_{membrane}$. The real PS value for the MBEC4 monolayer (PS_{trans}) was calculated from $1/PS_{app} = 1/PS_{membrane} + 1/PS_{trans}$. The PS_{trans} values were divided by the surface area of the Transwell^{TM} inserts to generate the permeability coefficient (P_{trans}, in cm per min).

Cellular Uptake of Quinacrine by MBEC4 Cells

For the uptake experiments, MBEC4 cells were washed three times with uptake buffer (143 mM NaCl, 4.7 mM KCl, 1.3 mM $CaCl_2$, 1.2 mM $MgSO_4$, 11 mM D-glucose,